Electromagnetic core-mantle coupling for laterally varying mantle conductivity

Johannes Wicht, Dominique Jault

JOURNAL OF GEOPHYSICAL RESEARCH, VOL. 105, NO. B10, PAGES 23,569–23,578, OCTOBER 10, 2000

Electromagnetic core-mantle coupling for laterally varying mantle conductivity

Johannes Wicht

Institut für Geophysik, Georg-August Universität, Göttingen, Germany

Dominique Jault

Laboratoire de Géophysique Interne et Tectonophysique, Université de Grenoble, Grenoble, France

Abstract. Electromagnetic coupling between the Earth's core and mantle is one of the proposed mechanisms to explain length of day (LOD) variations on decadal timescales. Mantle conductivity, a determining parameter in this process, is only poorly known. Earlier work on core-mantle coupling mostly assumed laterally homogeneous mantle conductivities. However, the lower mantle is a highly inhomogeneous region. Seismic evidence is growing that many of the inhomogeneities must have chemical, compositional, or thermal origins. We consider the effect of different laterally varying conductivity models on electromagnetic mantle torques. Torque amplitudes for a specific epoch can depend strongly on the assumed conductivity distribution. However, when comparing time series of the electromagnetic torque to decadal LOD variations, none of the examined conductivity models improve the agreement significantly. As in the simplest case of a homogeneous mantle conductivity, a minimum average conductance of 10^8 S is always required to make electromagnetic coupling efficient.

1. Introduction

The Earth's rotation period changes over a variety of different timescales [e.g., *Hide and Dickey*, 1991]. Most of the variation can be explained by coupling to the atmosphere and oceans, changes in the Earth's moment of inertia, or tidal friction. Length of day (LOD) variations on decadal timescales, however, are so large (of the order 10^{-7} s yr^{-1}) that only the core's moment of inertia is big enough to take the associated changes in angular momentum.

Three mechanisms seem capable of providing the required coupling of core and mantle: gravitational coupling between density and/or topographic inhomogeneities of inner core and mantle [*Buffett*, 1996a, 1996b; *Szeto and Xu*, 1997], topographic coupling from fluid pressure on a deformed core-mantle boundary (CMB) [*Hide*, 1986; *Jault and Le Mouël*, 1991; *Kuang and Bloxham*, 1996; *Jault and Le Mouël*, 1999], and Lorentz forces acting on the Earth's mantle. We will consider the third mechanism here.

Stix and Roberts [1984] introduced a method to determine the electromagnetic torque on the mantle based on the reasonable assumption that the mantle conductivity σ is much smaller than the core conductivity σ_c. The conductivity ratio $\epsilon = \sigma/\sigma_c$ can then serve as a small parameter in a perturbation analysis that leads to torque expressions of first order in ϵ. In addition to a mantle conductivity model, information on the magnetic field, its secular variation (SV), and the toroidal potential field Φ of $(\mathbf{U}B_r)$ is required for the torque calculation. $(\mathbf{U}B_r)$ is the product of the horizontal velocity and the radial magnetic field at the core surface. Its poloidal/toroidal decomposition reads

$$(\mathbf{U}B_r) = \nabla_H \Psi + \nabla\times(\mathbf{r}\Phi) \ , \qquad (1)$$

where ∇_H is the horizontal part of the gradient operator.

Subsequent papers [*Stix and Roberts*, 1984; *Love and Bloxham*, 1994; *Stewart et al.*, 1995] used core flow inversions to determine Φ and assumed a laterally homogeneous mantle conductivity. The torque's time dependence resulting from these forward calculations does not agree with LOD variations. Moreover, a consistently negative offset Γ_0 of the calculated torque variation was found, while the LOD torques oscillate around a zero mean. Some authors report an additional long timescale trend that also distinguishes forward models and decadal LOD data [*Stewart et al.*, 1995; *Holme*, 1998a]. Both deviations are usually attributed to the neglected electromagnetic diffusion, that can give rise to a slowly varying torque contribution [*Stix and Roberts*, 1984].

However, *Holme* [1998a] proved that electromagnetic coupling is nevertheless capable of explaining LOD vari-

Paper number 2000JB900176.
0148-0227/00/2000JB900176$09.00

ations, provided the required torque is used as an internal constraint in the flow inversion. Consequently, these type of calculations are called inverse models. Flow inversions are known to be nonunique [*Backus,* 1968] and therefore potentially leave freedom for additional constraints. For a mantle conductance of at least $C = 10^8$ S the LOD variation can be reproduced without unreasonable forcing (changing, deforming) the core surface flow [*Holme,* 1998b]. Conductance is defined as the radially integrated mantle conductivity.

Wicht and Jault [1999] (hereinafter referred to as WJ1) introduced an alternative method to determine the toroidal potential field Φ of $(\mathbf{U}B_r)$. Their method relies on the fact that the poloidal and toroidal parts of $(\mathbf{U}B_r)$ have to cancel on null-flux lines and has therefore been dubbed the NFL method. Null-flux lines are lines where the radial magnetic field vanishes at the core-mantle boundary. The poloidal part of $(\mathbf{U}B_r)$ is given by the secular variation via the radial induction equation in the frozen flux approximation, i.e., neglecting magnetic diffusion in the core:

$$\dot{B}_r = -\nabla\cdot(\mathbf{U}B_r) = -\nabla_H^2 \Psi \ . \qquad (2)$$

We thus know Φ where B_r vanishes and can use this information to construct a global model for Φ. While these calculations bypass the inherent indeterminacy of flow inversions, errors in NFL position and the NFL coverage of the CMB are issues. The results of WJ1 were similar to those based on flow inversions: LOD variations could only be reproduced if the torque is used as a constraint in the inversion and the mantle conductance exceeded $C = 10^8$ S. Here we will rely on the NFL method only. However, the results of WJ1 and some numerical experiments not presented here suggest that the methods of including a lateral conductivity variation and the qualitative results presented would hold as well, if core flow inversions were the basis for the Φ models.

A conductance of $C = 10^8$ S is not compatible with recent conductivity estimates of lower mantle material based on geochemical laboratory experiments [*Shankland et al.,* 1993; *Katsura et al.,* 1998]. To be sufficiently efficient, electromagnetic coupling thus has to rely on a possibly higher conductivity of a chemically or compositionally differentiated lower mantle layer. For example, a layer of 100 km thickness and a conductivity of 10^3 S m^{-1} would yield the required conductance.

Seismic explorations have shown that the lower mantle is a highly inhomogeneous region [*Su et al.,* 1994; *van der Hilst et al.,* 1997; *Liu et al.,* 1998; *Ishii and Tromp,* 1999]. A well-established anisotropic layer is D'' extending to $\sim$ 200 km above the CMB [e.g. *Lay et al.,* 1998], and recently ultra low velocity zones (ULVZ) have been found in the bottom 50 km of the mantle [*Garnero et al.,* 1998]. In addition, a third layer extending up to a depth of 1700 km has been proposed by *van der Hilst and Kárason* [1999]. All three layers show pronounced lateral variations and seismic signals that cannot be explained by thermal effects alone [*van der Hilst et al.,* 1997; *Lay et al.,* 1998]. Thus variations in chemical composition have been suggested. In particular, partial melting and enrichment with iron alloys have been proposed for the ULVZ. This would diminish seismic velocities and potentially increase the conductivity [*Li and Jeanloz,* 1991; *Manga and Jeanloz,* 1996]. On the other hand, *Poirier and Le Mouël* [1992] state that percolation of iron from the core into the mantle can only be marginal.

Another interesting issue, thought to be connected to lateral conductivity variations in the mantle, is the question of preferred virtual dipole paths (VDPs) during geomagnetic reversals [*Laj et al.,* 1991]. *Runcorn* [1992] proposed that the electromagnetic torque could force the magnetic poles to follow the observed preferred VDPs if the mantle conductivity is considerably higher beneath the Pacific than in other mantle regions. Interestingly, global seismic models [*Liu et al.,* 1998; *Ishii and Tromp,* 1999] show decreased velocities in the lower mantle beneath the Pacific, and this is also an area where a ULVZ can be found [*Garnero et al.,* 1998]. However, *Brito et al.* [1999] demonstrate that the magnetic pole trajectory is not strongly affected by lateral conductivity variations, assuming the field stays mainly dipolar during the reversal.

Recently, the effect of lateral conductivity variations on electromagnetic core-mantle coupling has been considered by *Holme* [2000]. He examines the question whether any conductivity variation could diminish the mean torque Γ_0 and eliminate the long timescale trend. We try to clarify the effect of lateral conductivity variations more generally and, while *Holme* [2000] employs forward calculations, will concentrate on the inverse approach. In section 2 we describe the methods used to calculate the electromagnetic torque. Section 3 will show that the electrical potential in the lower mantle does not depend significantly on the assumed lateral conductivity distribution. Neglecting this dependence simplifies the problem and allows us to explore different conductivity models. We end with a discussion.

2. Torque Calculation

2.1. Methods and Numerics

Electromagnetic coupling is caused by Lorentz forces acting on electric currents in the mantle:

$$\Gamma = \int dV \ \sin\theta\,[\mathbf{j}\times\mathbf{B}]_\phi \ . \qquad (3)$$

Here we consider only the torque component in direction of the rotation axis, which is responsible for length of day changes. The integral has to be taken over the conducting part of the mantle; $\mathbf{j}$ is the current density and $\mathbf{B}$ is the Earth's magnetic field. *Roberts* [1972] named the torque caused by the action of $\mathbf{B}$ on a poloidal (toroidal) current density the toroidal (poloidal) torque, based on the geometry of the magnetic field produced by the current.

Time variation of the poloidal geomagnetic field,

$$\mathbf{B} = \nabla\times\nabla\times(\mathbf{r}S) \ , \tag{4}$$

induces a toroidal electric field,

$$\mathbf{E}_t = -\nabla\times(\mathbf{r}\dot{S}) \ , \tag{5}$$

while gradients of the electric potential V in the mantle can be identified with a poloidal electric field,

$$\mathbf{E}_p = -\nabla V \ . \tag{6}$$

Here S is the poloidal magnetic potential field.

Ohm's law connects electrical field and current: $\mathbf{j} = \sigma\,\mathbf{E}$. Hence, for a laterally homogeneous mantle conductivity, poloidal and toroidal current densities are respectively associated with electric fields of the same type. This does not hold when the conductivity varies laterally.

Since we regard the distinction of the two electric field sources to be more relevant than the involved current types, we separate the electromagnetic torque into a contribution related to secular variation,

$$\Gamma_{\rm sv} = -\int dV\, r\sin\theta\,\sigma\,\left[(\nabla\times(\mathbf{r}\dot{S}))\times\mathbf{B}\right]_\phi \ , \tag{7}$$

and a contribution connected with the electric potential,

$$\Gamma_{\rm pot} = -\int dV\, r\sin\theta\,\sigma\,\left[(\nabla V)\times\mathbf{B}\right]_\phi \ . \tag{8}$$

Once a mantle conductivity is assumed, the first contribution (7) can be calculated directly from a given field model and its time variation; we use UFM1 by *Bloxham and Jackson* [1992] throughout this paper. To calculate the second contribution (8), which turns out to be typically larger than the first one (WJ1), the electrical potential must be determined.

The condition that the divergence of the current density vanishes defines a second-order differential equation that we solve for the potential:

$$\nabla\cdot[\sigma\,\nabla V] = -\nabla\cdot\left[\sigma\,\nabla\times(\mathbf{r}\dot{S})\right] \ . \tag{9}$$

The radial current has to be zero at the boundary between the conducting and insulating part of the mantle. This serves as the first boundary condition for (9), while the second one is the continuity of the horizontal electric field at the CMB. In the frozen flux approximation this condition is fulfilled for

$$V = r_0\,\Phi \ , \tag{10}$$

where r_0 is the core radius. The field Φ has to be determined first and can then serve as a boundary condition for (9). Throughout this paper we use the NFL method to invert for models of Φ; details of this procedure are given by WJ1.

We expand the variables V, Φ, and the conductivity σ in spherical harmonics:

$$V(r,\theta,\phi) = \sum_{l=0}^{l=\infty}\sum_{m=0}^{m=l} V_{lm}(r)\,P_l^m(\theta)\,e^{(im\phi)} + \text{c.c.} \ , \tag{11}$$

$$\Phi(\theta,\phi) = \sum_{l=0}^{l=\infty}\sum_{m=0}^{m=l} \Phi_{lm}\,P_l^m(\theta)\,e^{(im\phi)} + \text{c.c.} \ , \tag{12}$$

$$\sigma(r,\theta,\phi) = \sum_{l=0}^{l=\infty}\sum_{m=0}^{m=l}\sum_{n=1}^{n=\infty}\left\{\sigma_{lmn}\,P_l^m(\theta)\,e^{(im\phi)}\left(\frac{r_0}{r}\right)^{\alpha_n}\right\} + \text{c.c.} \ , \tag{13}$$

where the $P_l^m(\theta,\phi)$ are Schmidt normalized associated Legendre polynomials of degree l and order m; c.c stands for the complex conjugate. Note that the complex coefficients $V_{lm}(r)$ depend on the radius r, while we have used a power law ansatz to describe the radial dependence of the conductivity. Analogous spherical coefficients for the poloidal magnetic field potential S and its radial dependence are given by the magnetic field model UFM1 [*Bloxham and Jackson*, 1992] employed here.

Equation (9) as well as the boundary conditions are transferred from physical (θ,ϕ) space into functional (l,m) space by inserting the expansions, multiplying by a spherical harmonic $P_l^m(\theta)\,e^{(im\phi)}$, and integrating over a spherical surface. The orthogonality of the spherical harmonics is used in this process. Boundary condition (10) then reads $V_{lm}(r_0) = r_0\Phi_{lm}$.

Equation (9) transforms into a system of second-order differential equations in radius for the coefficients $V_{lm}(r)$. Suppose that the expansions in l are truncated at orders L_V, L_Φ, L_σ, and L_S, respectively. Using a magnetic field model and assuming a conductivity distribution determines the right-hand side of (9), which is of order $L = L_\sigma + L_S + 1$ in (l,m) space. Thus a system of equations of order L opposes the unknown electrical potential of order L_V. Standard least squares methods are used to solve this in general nonquadratic system. Depending on the conductivity model, the equation system can be truncated, down to $L = L_S + 1$ in some cases.

If the conductivity depends on radius only (9) can be solved analytically for each spherical harmonic coefficient V_{lm} [*Stix and Roberts*, 1984]. In the more general case of a laterally varying conductivity we employ central differences for the radial dependence. Since this dependence is generally weak close to the CMB, where the mantle conductivity and thus most of the torque action is concentrated, about $n_r = 10$ grid points suffice for the conductivity models explored here. Convergence in L and n_r have been checked for the solutions presented here, and numerical errors are smaller than 0.1%.

2.2. Conductivity Models

In order to focus on the influence of lateral conductivity variation we will keep the radial dependence fixed. Most likely, the mean mantle conductivity decays away from the core mantle boundary. WJ1 chose $\alpha_n = 9$ for a laterally homogeneous conductivity stretching throughout the mantle but found the resulting magnetic times τ_l [*Braginskiy and Fishman,* 1976] to be too long. To first order (in ϵ), τ_l is the time a magnetic signal of order l needs to diffuse through the mantle. Here we adopt a radially homogeneous conductivity ($\alpha_n = 0$), which is confined close to the CMB. This not only simplifies the problem: Since the magnetic time depends quadratically on the thickness δ of the conducting layer, τ_l will be considerably smaller than in WJ1. For example, for a layer of thickness $\delta = 200\,\mathrm{km}$ and homogeneous conductivity of $\sigma_0 = 1000\,\mathrm{S\,m^{-1}}$ we find $\tau_1 = 0.8\,\mathrm{years}$, a value that can be neglected compared to LOD variations with a typical timescale of 30 years. Note that we do not use the thin layer approximation employed by other authors [*Stewart et al.,* 1995; *Holme,* 1998a].

Information about lower mantle conductivity distribution is scarce, and the correlation between seismic velocities and conductivity variations remains unclear. However, in order to have a conductivity distribution that is at least based on some geophysical data we adopt the degree 16 model of *Liu et al.* [1998] at a depth of 2800 km and identify lower than average seismic velocity with higher than average conductivity. The conductivity is assumed to scale linearly with the seismic velocity for simplicity. This procedure defines the relative amplitudes σ_{lm} but leaves the mean conductivity σ_0 and an absolute variation amplitude σ_1 as free parameters. The resulting conductivity variation is shown in Figure 1.

In addition, we use two simplified models to explore the dependence of electromagnetic coupling on lateral conductivity variations more generally. In the one-mode model, lateral dependence is described by a single spherical harmonic:

$$\sigma = \sigma_0 + \sigma_1 \; N_l^m \; P_l^m(\cos\theta) \; \cos\left(\, m[\phi + \lambda]\right) \;, \quad (14)$$

where λ is a shift in longitude ϕ. The normalization factor N_l^m guarantees that $\max\{N_l^m \; P_l^m(\cos\theta)\} = 1$. Six parameters characterize this model: the homogeneous conductivity σ_0, the variation amplitude σ_1, order l and degree m of the variation, the shift λ, and the thickness δ of the conducting layer.

In the localized conductivity model we concentrate mantle conductivity in a block adjacent to the CMB. The radial thickness of the block is controlled by δ, while its lateral extension is defined by two opening angles between pairwise opposite great circles. The four corner points where pairs of great circles meet on a spherical surface form a rectangle, a square if the opening angles are identical. Let γ be the opening angle in the latitude direction and β be the second (orthogonal) one. As for the one-mode model the localized conductivity model is characterized by six parameters: thickness δ, the opening angles γ and β, latitude and longitude of the block's midpoint, and the homogeneous conductivity σ_1 of the block.

3. Results

The electromagnetic torque depends almost linearly on the mantle conductivity, provided the conductivity is concentrated close to the CMB and its lateral scales are not too small. There is the possibility of nonlinear behavior, since the electrical potential depends on the conductivity distribution (see (9)). However, we find this dependence to be weak for the models explored here.

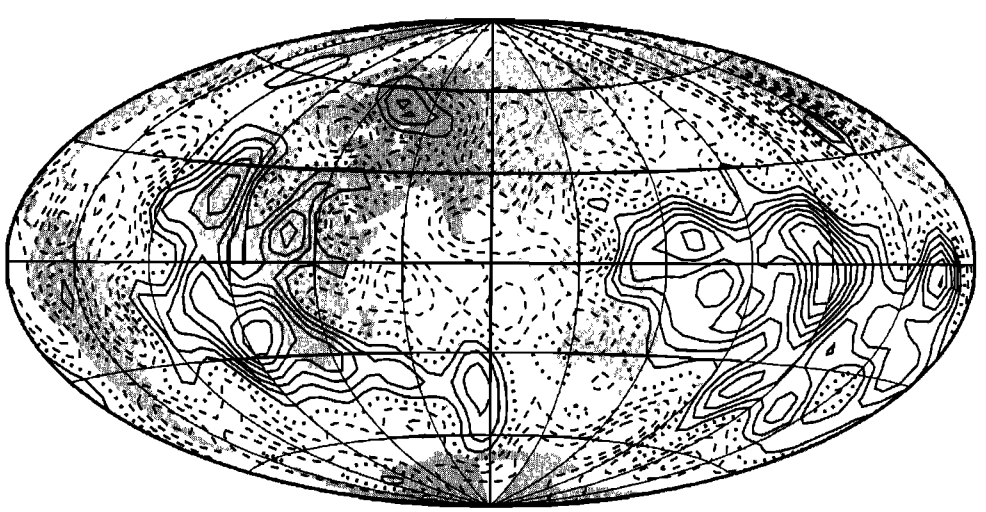

Figure 1. Contour lines for a lateral conductivity variation at the CMB inferred from a seismic degree 16 model by *Liu et al.* [1998]. High-conductivity zones (solid lines) have been identified with slow seismic velocities and vice versa. We use a Hammer equal-area projection for all spherical surface projections presented here and draw the continents for orientation.

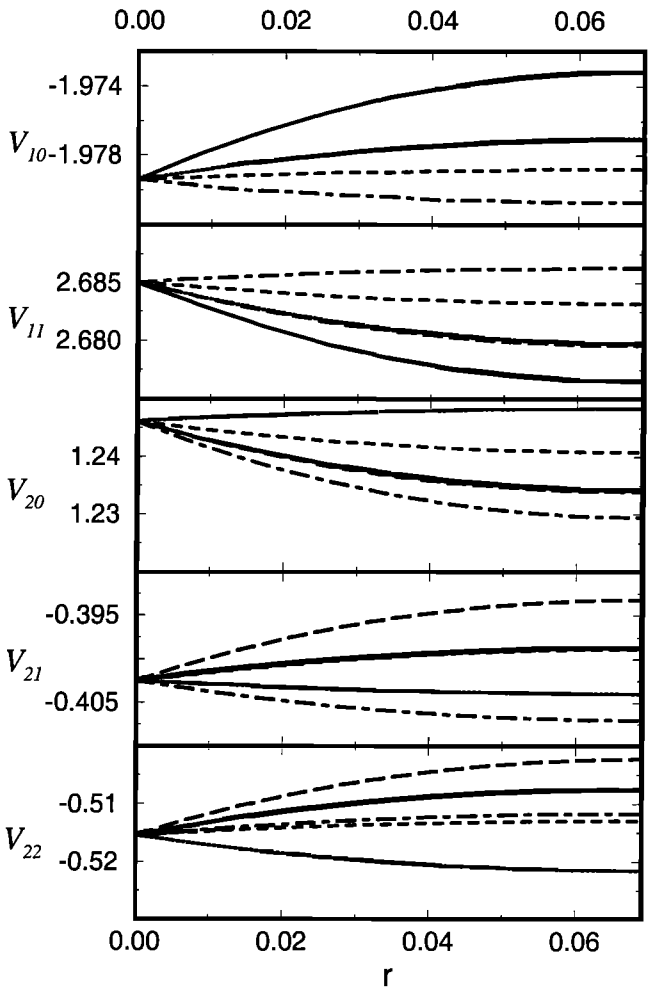

Figure 2. Radial dependence of the electrical potential V in the mantle. Real parts of different coefficients from an expansion in spherical surface harmonics are shown. Different one-mode models have been assumed for the conductivity: homogeneous conductivity ($l = 0$, $m = 0$) solid line, ($l = 1$, $m = 0$) dotted line, ($l = 1$, $m = 1$) dashed line, ($l = 2$, $m = 0$) long dashed line, and ($l = 2$, $m = 2$) dash-dotted line. Mean conductivity σ_0 and variation amplitude σ_1 are 10^3 S m^{-1}. The thickness of the conducting layer is $\delta = 200$ km. The latitude shift λ has been chosen individually to maximize the effect of each conductivity variation. Labels on the x-axis indicate the radius in units of mantle thickness. Only the conducting layer is shown here.

Close to the CMB, where the conductivity and thus most of the torque action is concentrated, the potential is determined by the value of the toroidal part of $(\mathbf{U}B_r)$ via boundary condition (10). Therefore the potential has the same value at the CMB, no matter which mantle conductivity is assumed. Figure 2 shows the radial dependence of different potential harmonics V_{lm} in the conducting part of the mantle. This dependence is always weak, and the harmonics never deviate much from the solution for a homogeneous mantle conductivity.

In Figure 3 we show the dependence of the electromagnetic torque on the relative amplitude of lateral conductivity variation σ_1/σ_0 for different one-mode models and the magnetic field model UFM1 for 1990. The torque scales linearly with the variation amplitude and can vary by a factor of 2 depending on the assumed conductivity model. Solid circles in Figure 3 represent solutions where the lateral conductivity variation has been ignored in calculating the electric potential via (9). The error of this linear approximation grows with increasing conductivity variation amplitude σ_1 and decreasing horizontal conductivity scales. The maximum deviation between linear and nonlinear solutions in Figure 3 is $\sim$ 1% for ($l = 2, m = 2$) and $\sigma_1/\sigma_0 = 1$. For the most complicated conductivity structure employed here, the seismically inferred variation of degree 16 shown in Figure 1, the error is also about $\sim$ 1%, again for UFM1 1990. We are thus confident in using the analytical potential for a laterally homogeneous mantle conductivity when exploring the dependence of the electromagnetic torque on various conductivity variations presented below.

This linear approximation might seem problematic in the context of the localized conductivity models. However, we assume implicitly that the conductivity gradients are small enough to validate the approximation in the potential calculation and large enough to justify using a block of conducting material in the torque calculation.

WJ1 have shown that for a laterally homogeneous mantle conductivity most of the torque action for 1990 is concentrated beneath Africa and the mid-Atlantic.

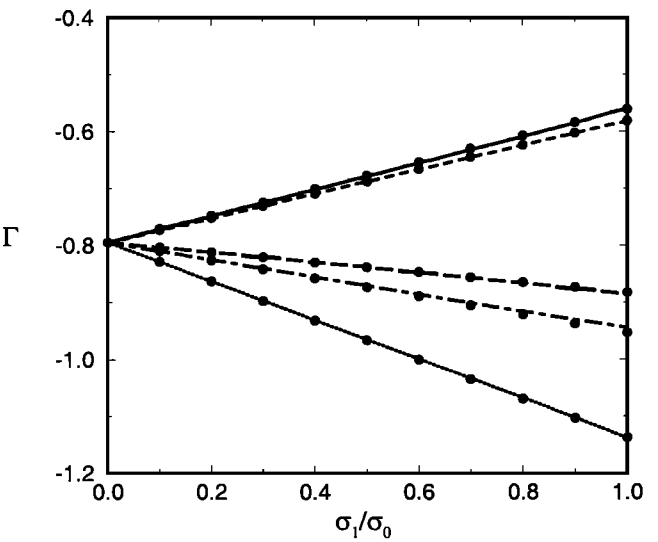

Figure 3. Dependence of the total electromagnetic torque on the conductivity variation amplitude σ_1 for different one-mode models: ($l = 1$, $m = 0$) solid line, ($l = 1$, $m = 1$) dotted line, ($l = 2$, $m = 0$) dashed line, ($l = 2$, $m = 1$) long dashed line, ($l = 2$, $m = 2$) dash-dotted line. Solid circles represent results where the electric potential for a laterally homogeneous conductivity has been used. Agreement between these approximations and the exact solutions is always better than 1%. Conductivity parameters are the same as for Figure 2.

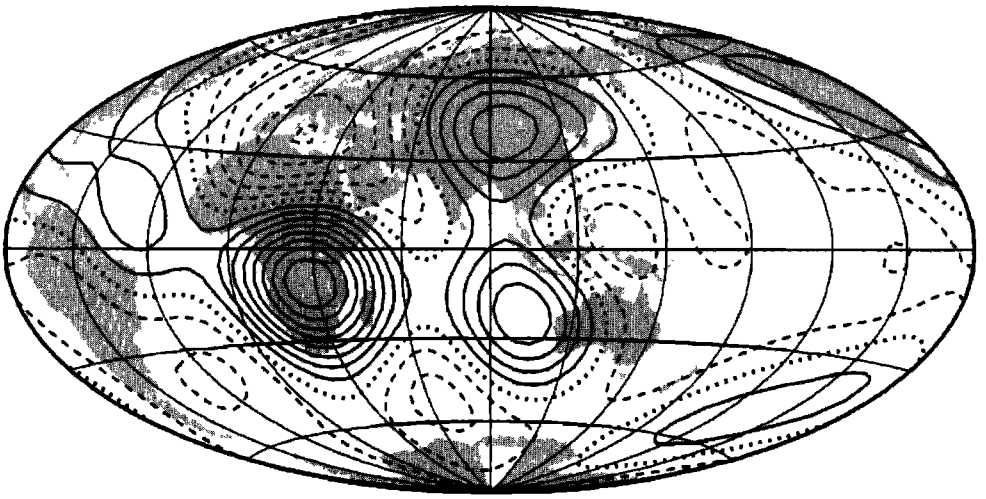

Figure 4. Contour lines of the misfit M_{LOD} to torques explaining length of day variations for the time span from 1900 to 1990 in 2.5-year steps. To derive this plot, the mantle has been scanned with a conductivity of $10^4\,\mathrm{S\,m^{-1}}$, concentrated in a block adjacent to the CMB with a thickness of $\delta = 200\,\mathrm{km}$ and a lateral extension of $\beta = \gamma = 20°$. The resulting M_{LOD} value has then been plotted at longitude and latitude of the block's midpoint. Resolution corresponds to spherical harmonics up to degree and order 6. Misfit values are generally high, ranging from a minimum of $M_{\mathrm{LOD}} = 0.83$ to a maximum of $M_{\mathrm{LOD}} = 1.74$. These values can not be decreased significantly by further increasing the conductivity. The dotted line denotes the mean M_{LOD} level. Solid lines mark larger than mean, and dashed lines mark smaller that mean levels.

The torque amplitude depends on the overlap between the conductivity maxima and this area. In the one-mode model the longitude shift λ can be chosen to maximize the absolute torque amplitude, but the latitude of the conductivity maximum is fixed for a given Legendre polynomial. These effects explain the different gradients found in Figure 3 and the torques dependence on λ (not shown here).

The localized conductivity model allows to explore the effect of concentrating (or increasing) the conductivity in different areas of the deep mantle. Figure 4 and Figure 5 show the results of scanning the mantle with a conducting block of thickness $\delta = 200\,\mathrm{km}$ and a lateral extension of $\beta = \gamma = 20°$. The conductivity is $\sigma_1 = 10^4\,\mathrm{S\,m^{-1}}$ to maximize the effect, not claiming to be realistic. UFM1 has been used in 2.5-year steps from 1900 to 1990. The contour lines in Figure 4 represent the misfit M_{LOD} between length of day torques Γ_{LOD} and the total electromagnetic torque $\Gamma = \Gamma_{\mathrm{SV}} + \Gamma_{\mathrm{pot}}$,

$$M_{\mathrm{LOD}} = \sqrt{\frac{\sum_{i=1}^{N}[\Gamma_{\mathrm{LOD}}(t_i) - (\Gamma(t_i) - \Gamma_0)]^2}{\sum_{i=1}^{N}\Gamma_{\mathrm{LOD}}^2(t_i)}}\,. \quad (15)$$

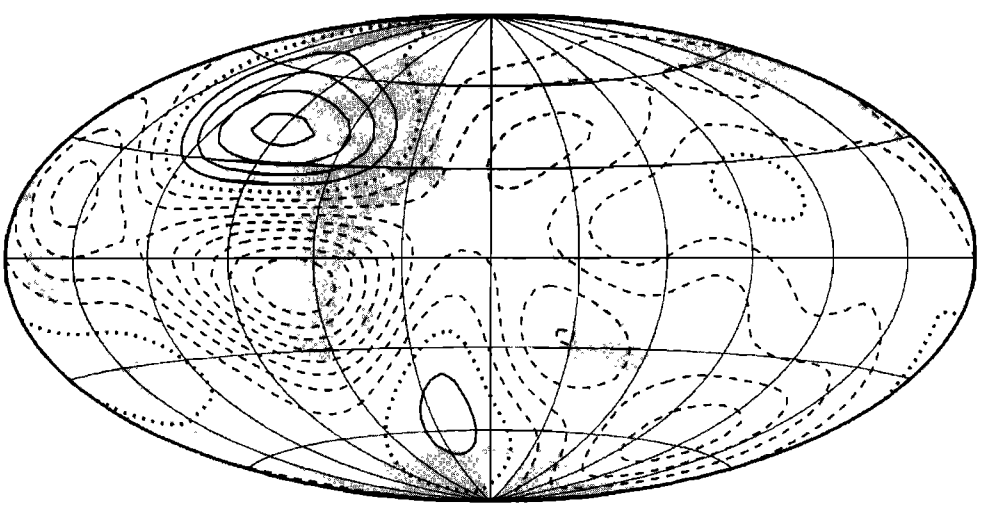

Figure 5. Contour lines represent the temporal mean electromagnetic torque Γ_0 from 1900 to 1990 for a scan with the localized conductivity model. The maximum is $\Gamma_0 = 0.40 \times 10^{18}\,\mathrm{N\,m}$ and the minimum is $\Gamma_0 = -1.13 \times 10^{18}\,\mathrm{N\,m}$. Parameters and plotting methods are the same as for Figure 4.

The sum is taken over all years (t_i, $i = 1, ..., N$) for which the calculation has been performed. Torques have been shifted by the mean torque values Γ_0 presented in Figure 5:

$$\Gamma_0 = \sum_{i=1}^{N} \Gamma(t_i) / N \quad . \tag{16}$$

These values are treated as an offset here because LOD torques oscillate around a zero mean.

The calculations do not even vaguely resemble LOD variations. Even the minimum misfit of $M_{\mathrm{LOD}} = 0.83$ is extraordinarily large, keeping in mind that for a zero torque $M_{\mathrm{LOD}} = 1$. A maximum value of $M_{\mathrm{LOD}} = 1.74$ is reached when concentrating the conductivity beneath southern Africa. This area always contributes significantly to the electromagnetic torque values throughout the century (WJ1) because of the typical strong westward core surface flows and the relatively strong radial magnetic field found here. Figure 5, showing contour lines of the offset Γ_0 resulting from the different conductivity locations, demonstrates that this region is also correlated with a strong negative offset. Concentrating the conductivity beneath the Pacific, on the other hand, could result in a zero mean torque. The fact that *Holme* [2000] can find a conductivity distribution yielding $\Gamma_0 = 0$ corresponds nicely with this result.

While it seems unlikely that the whole mantle conductivity is concentrated locally [*Poirier and Le Mouël*, 1992], Figure 4 can nevertheless serve as a model for a somewhat optimized conductivity variation if we reduce (increase) an average conductivity where large (small) misfits are found. To maximize the effect we chose $\sigma_1 = \sigma_0$. Table 1 presents LOD misfits and mean torques for such a conductivity model in comparison with values for a laterally homogeneous conductivity, a conductivity variation inferred from a seismic model

Table 1. Misfit M_{LOD} and offset Γ_0 to LOD torques

Conductivity Model	σ_0[a]	σ_1[a]	M_{LOD}	Γ_0[b]
Homogeneous	2×10^3		1.42	−1.74
Optimized[c]	2×10^3	2×10^3	1.32	−1.30
Seismic[d]	2×10^3	2×10^3	1.38	−1.70
Pacific[e]		10^4	1.35	−0.97

[a] Mean conductivity σ_0 and variation amplitude σ_1 are given in $\mathrm{S\,m^{-1}}$. They have been chosen to make the RMS variation from 1900 to 1990 of torques Γ_{LOD} that would explain LOD variation and the calculated electromagnetic torques comparable. Thickness of the conducting layer is $\delta = 200$ km in all cases.

[b] In 10^{18} N m

[c] Conductivity variation based in Figure 4.

[d] Conductivity variation inferred from a degree 16 seismic model by *Liu et al.* [1998].

[e] Conductivity concentrated in an area centered around 0° latitude and 202.5° longitude extending $\gamma = 70°$ and $\beta = 70°$ to mimic a possible ULVZ.

(Figure 1) and a conductivity concentration beneath the Pacific. The position of the latter is motivated by ULVZs found at the base of the mantle. While the ULZVs have a thickness of up to 50 km, we have kept $\delta = 200$ km for better comparability here. Concentrating the conductance closer to the CMB would slightly increase the electromagnetic coupling. Clearly, all misfit values presented in Table 1 are far too high.

We conclude that conductivity variation can have a significant effect on the torque amplitude and its temporal mean but does not alter the torque's time dependence in a way that would bring it significantly closer to the observed LOD variation. *Holme* [1998a] has shown with his inverse model that mainly the time dependence of the core surface flow is increased in order to reproduce LOD torques. This would explain why static conductivity variations can not improve the results. On the other hand, *Celaya and Wahr* [1996] demonstrate that the smaller-scale velocity components may be more time-dependent than the larger ones, and we find this to be also true for the Φ field in our formalism. Small-scale conductivity variations enhance the contribution of small Φ scales to the electromagnetic torque and thus increase its time dependence. However, the time dependence does not follow the LOD signal, and the misfit remains large.

We therefore follow *Holme* [1998a] and WJ1's example and use the LOD torque as a constraint in the inversion for the toroidal potential Φ of $(\mathbf{U}B_r)$. These calculations have been shown to be successful for laterally homogeneous mantle conductivities, that is, the torque can be reproduced with the resulting Φ field. Naturally, Φ is altered by the additional condition, and the changes only stay in an acceptable range if the mantle conductance is of the order 10^8 S. With this kind of inversion it is hard to define what "acceptable" really means. WJ1 have used two measures: the misfit of the solution to the input "data" and the roughness of the resulting Φ field.

In the case of the NFL method the misfit M_{NFL} measures how well the poloidal and toroidal part of $(\mathbf{U}B_r)$ cancel on null flux lines. The poloidal part is given by the SV (equation (2)) and represents the "data" input. The roughness is measured by

$$R = r_{\mathrm{CMB}}^4 \int_{\mathrm{CMB}} d\Omega \left[(\nabla_H^2 \frac{\partial \Phi}{\partial \theta})^2 + (\nabla_H^2 \frac{1}{\sin\theta} \frac{\partial \Phi}{\partial \phi})^2 \right] ,$$

which has been chosen by analogy with the methods used in flow inversion by *Bloxham* [1988] and others. Here $d\Omega$ is a spherical surface element. WJ1 minimize M_{NFL} and R simultaneously in a least squares inversion to solve for Φ. (Note that in WJ1, Table 5, the symbol $N^{(3)}$ has been used instead of R, and the values have been scaled by 10^{10}.) The global nature of R makes it the more severe and more relevant measure (WJ1). We will therefore mainly rely on R, while LOD and NFL misfits are generally small for the results presented below.

Figure 6 shows contour lines of R for a scan with the localized conductivity model, again using the values and

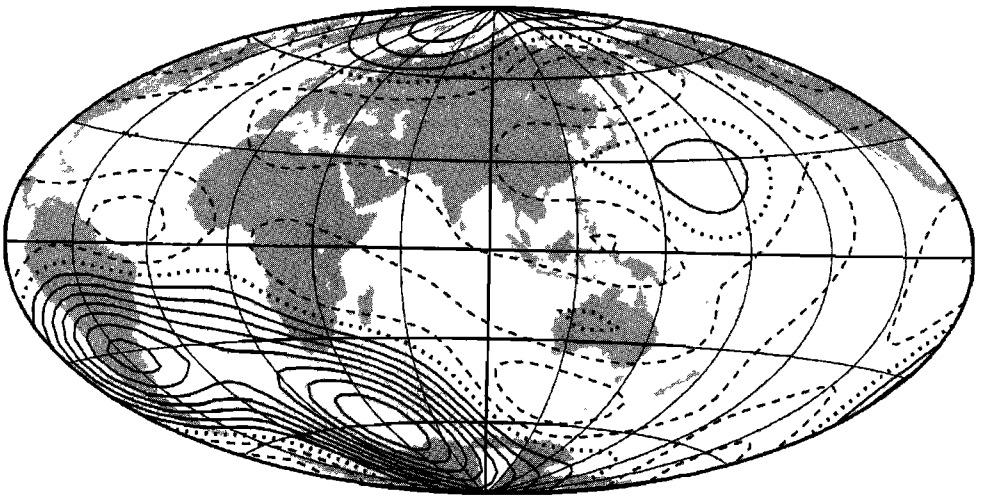

Figure 6. Contour lines of the Φ field roughness R, again for the same localized conductivity scan as in figure 4. Temporal mean values from 1900 to 1990 in 2.5-year steps are shown. The Φ field is now enforced to reproduce LOD torque values. Large R values signify that the required distortion is stronger, and Φ probably unreasonably complex. The roughness spans values from $R = 9.87 \times 10^9$ to $R = 6.72 \times 10^{11}$. Contour interval is 6.03×10^{10}.

the formalism introduced above (see Figure 4 caption). Lateral variations of M_{LOD} and M_{NFL} are very similar to Figure 6. The LOD misfit M_{LOD} lies between 0.11×10^{-3} and 0.76×10^{-2}. Using the variation displayed in Figure 6 as an optimized conductivity distribution, we can now explore for which values of σ_0 and σ_1 the roughness stays reasonable.

Figure 7 shows the dependence of R on the horizontally averaged conductance for two values of the variation amplitude σ_1. For the larger value the influence of geostrophy as an additional constraint in the Φ inversion is demonstrated (WJ1). Also, results for a homogeneous and the seismically inferred conductivity are presented. The influence of the conductivity variation is only marginal. Asymptotic roughness values are approached for large conductances. For the optimized conductivity model these values lie closer to the values $R = 0.93 \times 10^{10}$ for the Φ field not forced to reproduce LOD torques. The highest asymptotic value is found for the geostrophic solutions. However, a conductance of $C = 10^8$ S seems to mark the point where all models reach the asymptotic regime. We no longer support the conclusion of WJ1 that geostrophic inversions require higher conductances. WJ1 had calculated only a few of the points presented in Figure 7, and judged the acceptable conductance based on absolute R values rather than on the asymptotic behavior. This correction is independent from the lateral variation of conductivity.

4. Discussion

The dependence of the electromagnetic torque on various lateral conductivity distributions has been explored. Because of our poor knowledge of mantle conductivity we have taken the freedom to assume simplified and idealized models in addition to a conductivity distribution inferred from seismic studies.

The forward calculation, i.e., using a given magnetic field model, its secular variation, and a precomputed Φ field, showed that the electromagnetic torque amplitude depends strongly on the conductivity distribu-

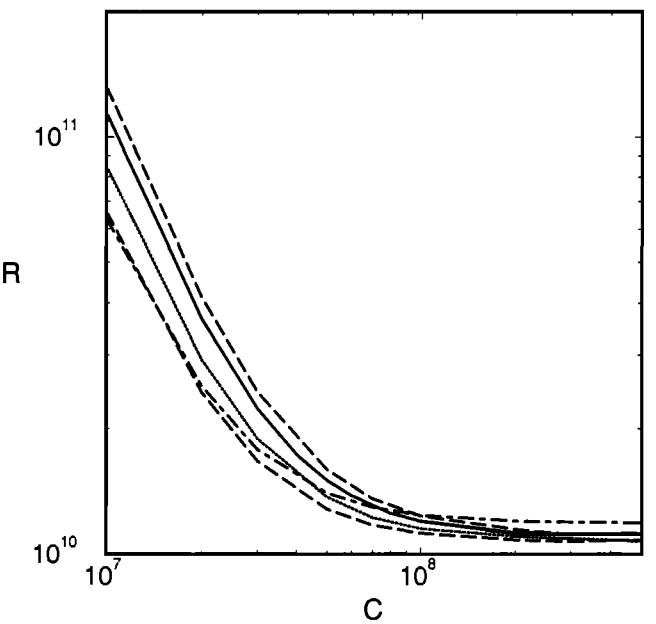

Figure 7. Dependence of the Φ field roughness R on the mantle conductance for different conductivity models. The solid line shows the results for a homogeneous conductivity. Dotted line and dashed line represent conductivity variations inferred from Figure 6 with $\sigma_1/\sigma_0 = 0.5$ and $\sigma_1/\sigma_0 = 1.0$ respectively. The long dashed line shows results for a variation based on the seismic model with $\sigma_1/\sigma_0 = 1.0$. Results represented by the dash-dotted line use the same conductivity model as for the dashed line, but in addition geostrophy has been enforced in the Φ inversion. In all cases a conducting layer of 200 km thickness has been assumed.

tion and may even change sign. However, for no conductivity model did we come close to reproducing the decadal length of day variation. The misfit can be reduced slightly for an appropriately chosen conductivity model but never significantly. The mean torque Γ_0 depends strongly on the assumed conductivity variation. This offset to the mean LOD torque is commonly attributed to the diffusive couple. Any estimate of this torque contribution is therefore only meaningful when based on a reasonable model of the lateral conductivity variation.

Inverse modeling shows that the average conductance has to be at least $C = 10^8$ S for the laterally conductivity variations tested here as well as for a laterally homogeneous conductivity [*Holme*, 1998b; *Wicht and Jault*, 1999]. (Note the corrected value for geostrophy in section 3.) The inherent indeterminacy of the core surface flow (or the Φ field) does not allow a distinction to be made between different conductivity models. The case is different for dynamo simulations that include electromagnetic coupling to the mantle. Here core flow and magnetic field are known, and lateral conductivity variations should be considered.

The required conductance of $C = 10^8$ S exceeds the values proposed for mantle material at lower mantle conditions [*Shankland et al.*, 1993; *Katsura et al.*, 1998]. Provided D'', ULVZs, or other heterogeneities in the lower mantle are correlated with higher conductivities, electromagnetic coupling may still be a possible explanation for decadal length of day variations. We have shown that lateral conductivity variations will then play an important role.

References

Backus, G.E., Kinematics of geomagnetic secular variation in a perfect conducting core, *Philos. Trans. R. Soc. Lond.*, on *Ser. A, 263*, 239-266, 1968.

Bloxham, J., The Determination of Fluid Flow at the Core Surface from Geomagnetic Observations, in *Mathematical Geophysics, A Survey of Recent Developments in Seismology and Geodynamics*, edited by N.J. Vaar et al., 189-208, D. Reidel, Hingham, MA, 1988.

Bloxham, J., and A. Jackson, Time-dependent mapping of the magnetic field at the core-mantle boundary, *J. Geophys. Res., 97*, 19,537-19,563, 1992.

Braginskiy, S.I., and V.M. Fishman, Electromagnetic coupling of the core and mantle when electrical conductivity is concentrated near the core boundary, *Geomagn. Aeron., 16*, 443-446, 1976.

Brito, D., J.M. Aurnou, and P.L. Olson, Can heterogeneous core-mantle electromagnetic coupling control geomagnetic reversals?, *Phys. Earth Planet. Inter., 112*, 159-170, 1999.

Buffett, B.A., Gravitational oscillations in the length of day, *Geophys. Res. Lett., 23*, 2279-2282, 1996a.

Buffett, B.A., A mechanism for decade fluctuations in the length of day, *Geophys. Res. Lett., 23*, 3803-3806, 1996b.

Celaya, M., and J. Wahr, Aliasing and noise in core-surface flow inversions, *Geophys. J. Int., 126*, 447-469, 1996.

Garnero, E.J., J. Revenaugh, Q. Williams, T. Lay, and L.H. Kellog, Ultralow velocity zone at the core-mantle boundary, in *The Core-Mantle Boundary Region, Geodyn. Ser.*, vol. 28, edited by M. Gurnis et al., pp. 167-180, AGU, Washington D.C., 1998.

Hide, R., The Earth's differential rotation, *Q. J. R. Astron. Soc., 278*, 3-14, 1986.

Hide, R., and J.O. Dickey, Earth's variable rotation, *Science, 253*, 629-637, 1991.

Holme, R., Electromagnetic core-mantle coupling, I, Explaining decadal changes in the length of day, *Geophys. J. Int., 132*, 167-180, 1998a.

Holme, R., Electromagnetic core-mantle coupling, II, Probing deep mantle conductance, in *The Core-Mantle Boundary Region, Geodyn. Ser.*, vol. 28, edited by M. Gurnis et al., pp. 139-151, AGU, Washington D.C., 1998b.

Holme, R., Electromagnetic core-mantle coupling, III, laterally varying mantle conductance, *Phys. Earth Planet. Inter., 117*, 329-344, 2000.

Ishii, M., and J. Tromp, Normal-mode and free-air gravity constraints on lateral variations in velocity and density of Earth's mantle, *Science, 285*, 1231-1236, 1999.

Jault, D., and J.-L. Le Mouël, Physical properties at the top of the core and core surface motions, *Phys. Earth Planet. Inter., 68*, 76-84, 1991.

Jault, D., and J.-L. Le Mouël, Comment on "On the dynamics of topographical core-mantle coupling" by Weijia Kuang and Jeremy Bloxham, *Phys. Earth Planet. Inter., 114*, 211-215, 1999.

Katsura, T., K. Sato, and E. Ito, Electrical conductivity of silicate perovskite at lower mantle conditions, *Nature, 395*, 493-495, 1998.

Kuang, W., and J. Bloxham, On the dynamics of topographical core-mantle coupling, *Phys. Earth Planet. Inter., 99*, 289-294, 1996.

Laj, C., A. Mazaud, R. Weeks, M. Fuller, and E. Herrero-Bervera, Geomagnetic reversal paths, *Nature, 351*, 447, 1991.

Lay, T., W. Quentin, and E.J. Garnero, The core-mantle boundary layer and deep Earth dynamics, *Nature, 392*, 461-467, 1998.

Li, X., and R. Jeanloz, Laboratory studies of the electrical conductivity of silicate perovskites at high pressures and temperatures, *J. Geophys. Res., 95*, 5067-5078, 1991.

Liu, X.-F., J. Tromp, and A.M. Dziewonski, Global analysis of shear wave velocity anomalies in the lowermost mantle, in *The Core-Mantle Boundary Region, Geodyn. Ser.*, vol. 28, edited by M. Gurnis et al., pp. 21-36, AGU, Washington D.C., 1998.

Love, J.J., and J. Bloxham, Electromagnetic coupling and the toroidal magnetic field at the core-mantle boundary, *Geophys. J. Int., 117*, 235-256, 1994.

Manga, M., and R. Jeanloz, Implications of a metal-bearing chemical boundary layer in D″ for mantle dynamics, *Geophys. Res. Lett., 23*, 3091-3094, 1996.

Poirier, J.-P., and J.-L. Le Mouël, Does infiltration of core material into the lower mantle affect the observed geomagnetic field?, *Phys. Earth Planet. Inter., 73*, 29-37, 1992.

Roberts, P.H., Electromagnetic core-mantle coupling, *J. Geomagn. Geoelectr., 24*, 231-259, 1972.

Runcorn, S.K., Polar path in geomagnetic reversals, *Nature, 356*, 654-656, 1992.

Shankland, T.J., J. Peyronneau, and J.-P. Poirier, Electrical conductivity of the Earth's lower mantle, *Nature, 366*, 453-455, 1993.

Stewart, D.N., F.H. Busse, K.A. Whaler, and D. Gubbins, Geomagnetism, Earth rotation and the electrical conductivity of the lower mantle, *Phys. Earth Planet. Inter., 92*, 199-214, 1995.

Stix, M. and P.H. Roberts, Time-dependent electromagnetic core-mantle coupling, *Phys. Earth Planet. Inter., 36*, 49-60, 1984.

Su, W.-J., R.L. Woodward, and A.M. Dziewonski, Degree

12 model of shear velocity heterogeneity in the mantle, *J. Geophys. Res., 100,* 9831-9852, 1994.

Szeto, A.M.K., and S. Xu, Gravitational coupling in a triaxial elipsoidal Earth, *J. Geophys. Res., 102,* 27,651-27,657, 1997.

van der Hilst, R.D., S. Widiyantoro, and E.R. Engdahl, Evidence for deep mantle circulation from global tomography, *Nature, 386,* 578-584, 1997.

van der Hilst, R.D., and H. Kárason, Compositional heterogeneity in the bottom 1000 kilometer of Earth's mantle: Toward a hybrid convection model, *Science, 283,* 1885-1891, 1999.

Wicht, J., and D. Jault, Constraining electromagnetic core-mantle coupling, *Phys. Earth Planet. Inter., 111,* 161-177, 1999.

D. Jault, LGIT, Université de Grenoble, BP53 38041 Grenoble CEDEX9, France.

J. Wicht, Institut für Geophysik, Georg-August Universität, Herzberger Landstrasse 180, 37075 Göttingen, Germany. (wicht@willi.uni-geophys.gwdg.de)

(Received December 1, 1999; revised April 7, 2000; accepted May 16, 2000.)